Magnetism

A relation between the resonance neutron peak and ARPES data in cuprates

by Ar. Abanov and Andrey V. Chubukov

Department of Physics, University of Wisconsin, Madison, WI 53706

We argue that the resonant peak observed in neutron scattering experiments on superconducting cuprates and the peak/dip/hump features observed in ARPES measurements are byproducts of the same physical phenomenon. We argue that both are due to feedback effects on the damping of spin fluctuations in a $d-$wave superconductor. We consider the spin-fermion model at strong coupling, solve a set of coupled integral equations for fermionic and bosonic propagators and show that the dynamical spin susceptibility below T_c possesses the resonance peak at $\Omega_{res} \propto \xi^{-1}$. The scattering of these magnetic excitations by electrons gives rise to a peak/dip/hump behavior of the electronic spectral function, the peak-dip separation is exactly Ω_{res}.

One of the most intriguing recent developments in the physics of high T_c materials is the realization that not only the normal but also the superconducting state of cuprates is not described by a weak coupling theory. In particular, ARPES experiments on Bi2212 have demonstrated [1, 2] that even in slightly overdoped cuprates at $T \ll T_c$, the spectral function $A(\mathbf{k}, \omega)$ near $(0, \pi)$ does not possess a single quasiparticle peak at $\omega = \sqrt{\Delta_{\mathbf{k}}^2 + \epsilon_{\mathbf{k}}^2}$, where $\Delta_{\mathbf{k}}$ is the superconducting gap and $\epsilon_{\mathbf{k}}$ is the fermionic dispersion. Instead, it displays a sharp peak which virtually does not disperse with k, a dip at frequencies right above the peak, and then a broad maximum (hump) which disperses with k and gradually recovers the normal state dispersion [1]. Simultaneously, the

neutron scattering experiments on near optimally doped $YBCO$ [3] and $Bi2212$ [4] at $T \ll T_c$ have detected a sharp resonance peak in the dynamical structure factor $S(q,\Omega) \propto \chi''(q,\Omega)$ centered at $q = Q = (\pi,\pi)$ and at frequencies ~ 40 meV.

Near optimal doping, the sharp peaks in $A(k,\omega)$ and in $S(Q,\Omega)$ both disappear above T_c, i.e., they both are clearly attributed to a superconductivity. In underdoped cuprates, $A(k,\omega)$ and $S(Q,\omega)$ keep displaying some superconducting features also above T_c [3]. In addition, in underdoped cuprates, the peak in the structure factor shifts to smaller frequencies and acquires some spin-wave like dispersion around $q = Q$ disappearing around $100meV$ which is roughly twice the peak frequency in $A(k_0,\omega)$ and in the density of states [5].

In this communication we show that the resonance peak in $S(Q,\Omega)$ and the peak/dip/hump features in $A(k,\omega)$ can be explained simultaneously by strong interaction between electrons and their collective spin degrees of freedom which near the antiferromagnetic instability are peaked at or near Q. Specifically, we demonstrate that a d-wave superconductor possesses *propagating* collective spin excitations at frequencies smaller than twice the maximum value of the $d-$wave gap. The propagating spin modes give rise to a sharp peak in $S(Q,\Omega)$ at $\Omega = \Omega_{res} \propto \xi^{-1}$ where ξ is the spin correlation length. The interaction with collective spin excitations yields the fermionic self-energy Σ_ω which at $T = 0$ has no imaginary part up to a frequency ω_0 which exceeds the measured superconducting gap by exactly Ω_{res}.

The phenomenon which we will describe is universal and does not depend on a particular model for cuprates. Indeed, consider the spin susceptibility $\chi(Q,\Omega)$ in a Fermi liquid which is somewhat close to a magnetic instability with momentum Q. Quite generally, $\chi^{-1}(Q,\Omega) \propto \xi^{-2} - \Pi_Q(\Omega)$ where $\Pi_Q(\Omega)$ subject to $\Pi_Q(0) = 0$ is the spin polarization operator (a fully renormalized particle-hole bubble). Assume that the Fermi surface geometry is such that a spin fluctuation with momentum Q can decay into a particle-hole pair (this implies that the Fermi surface contains hot spots). In the normal state, $\Pi_Q(\Omega)$ is then obviously linear in $i\Omega$. Consider now the superconducting state and suppose that the fermions near hot spots have a gap Δ. Then the decay process is forbidden until the spin frequency exceeds 2Δ. Kramers-Kronig rela-

tion implies that in this situation, $\Pi_Q(\Omega)$ at $\Omega < 2\Delta$ acquires a real part which quadratically depends on frequency: $\Pi_Q(\Omega) \propto \Omega^2$. Then $\chi^{-1}(Q,\Omega) \propto \xi^{-2} - \Omega^2$, i.e., near the antiferromagnetic instability, the spin susceptibility in a superconductor necessary possesses a resonance at $\Omega_{res} \propto \xi^{-1}$. Similar reasoning also explains the pseudoresonance peak observed in B_{1g} Raman scattering [7].

Consider now the fermionic propagator. In the absence of a resonance mode, the threshold for a fermionic decay due to scattering near hot spots is 3Δ. The resonance in the spin propagator opens up a new scattering channel with the threshold at a smaller frequency $\Delta + \Omega_{res}$. This frequency is still larger than Δ, i.e. the resonance does not affect a $\delta-$functional quasiparticle peak at $\omega = \Delta$. However, it gives rise to a dip in the spectral function at around $\Delta + \Omega_{res}$, because at larger frequencies the fermionic damping rapidly goes up. At even larger frequencies, the fermionic spectral function passes through a maximum (hump), and eventually goes down recovering the normal state behavior.

The rest of the paper is devoted to make these points more precise, and also to discuss a number of more subtle effects related to scattering of nearly antiferromagnetic spin fluctuations by fermions.

The point of departure for our analysis is the spin-fermion model for cuprates which is argued [8] to be the low-energy theory for Hubbard-type lattice fermion models. The model is described by

$$\begin{aligned} \mathcal{H} &= \sum_{\mathbf{k},\alpha} \mathbf{v_F}(\mathbf{k}-\mathbf{k}_F) c^\dagger_{\mathbf{k},\alpha} c_{\mathbf{k},\alpha} + \sum_q \chi_0^{-1}(\mathbf{q}) \mathbf{S_q} \mathbf{S_{-q}} + \\ & g \sum_{\mathbf{q},\mathbf{k},\alpha,\beta} c^\dagger_{\mathbf{k}+\mathbf{q},\alpha}\, \sigma_{\alpha,\beta}\, c_{\mathbf{k},\beta} \cdot \mathbf{S_{-q}} \,. \end{aligned} \tag{1}$$

Here $c^\dagger_{\mathbf{k},\alpha}$ is the fermionic creation operator for an electron with crystal momentum $\mathbf{k}$ and spin α, σ_i are the Pauli matrices, and g is the coupling constant which measures the strength of the interaction between fermions and the collective bosonic spin degrees of freedom. The latter are described by $\mathbf{S_q}$ and are characterized by a bare spin susceptibility $\chi_0(\mathbf{q}) = \chi_0\xi^2/(1+(q-Q)^2\xi^2)$.

Eq. (1) gives rise to fermionic and bosonic self-energies and is particularly relevant for fermions near hot spots – the points at the Fermi surface separated by Q. In cuprates, the hot spots are located near $(0,\pi)$

and symmetry related points. The presence of hot spots is essential for our consideration because the fermions near these points are mostly affected by the interaction with antiferromagnetic spin fluctuations, and at the same time, they produce the dynamical part of the spin propagator because a spin fluctuation with a momentum near Q can only decay into fermions near hot spots.

The normal state properties of the spin-fermion model have recently been analyzed and compared with the experiments [8, 9]. It was argued that the experimental situation in cuprates corresponds to a strong coupling limit $R = \bar{g}/v_F\xi^{-1} \gg 1$, where $\bar{g} = g^2\chi_0$ is the measurable effective coupling constant. The clearest experimental indication for this is the absence of the sharp quasiparticle peak in the normal state ARPES data for optimally doped and and underdoped cuprates [1, 2]. At strong coupling, a conventional perturbation theory does not work, but it turns out that a variant of perturbative expansion is still possible. The point is that at large R, there is a single self-energy diagram which depends only on frequency and scales as R, and infinite set of self-energy and vertex corrections diagrams which scale as powers of $\log R$ [8]. One can then incorporate the $O(R)$ term into the new zero-order theory and treat $\log R$ terms perturbatively, in the RG formalism. In practice, however, the prefactors for the $\log R$ vertex corrections are very small such that one can safely neglect these corrections except very near the antiferromagnetic transition. Below we just neglect vertex corrections and solve the problem in the self-consistent Born (i.e. FLEX) approximation.

An alternative computation procedure which we also executed is to formally treat the number of hot spots in the Brillouin zone $N = 8$ as a large number and perform $1/N$ expansion (one can verify that the RG expansion holds in $(1/N)\log R$). We checked that for finite ξ, both approaches yield equivalent results, However, in the limit $\xi = \infty$, the $1/N$ expansion is tricky and requires a special care. We therefore restrict here with the FLEX calculations and discuss $1/N$ expansion elsewhere [15].

The FLEX approximation is already highly nontrivial and has clear similarities with mean-field $d = \infty$ theories [10]: it incorporates the dominant ($\sim R$) self-energy correction which depends only on frequency, and also includes the dominant bosonic self-energy which gives rise to a fermionic damping. The corresponding set of self-consistent equations

is presented in Eq. (2) for a superconducting state. The normal state results are obtained by setting $\Delta = 0$.

The key physical effect which the FLEX theory describes is the progressive destruction, with increasing R, of the coherent quasiparticle peak. At the same time, the fermionic incoherence has no feedback on spin susceptibility which still has a simple relaxational form: $\chi^{-1}(q,\Omega) = \chi_0\xi^2/(1+(q-Q)^2\xi^2 - i\Omega/\omega_{sf})$ where $\omega_{sf} = (\pi/4)\ (v_F\xi^{-1})/R$ [8]. The absence of the feedback effect on spins is a quite general consequence of the fact that fermionic self-energy, albeit strong, has no dependence on the quasiparticle momentum [11].

In the superconducting state, this argument does not apply any more because superconducting and normal state Green's functions have different momentum dependences which can be interpreted as coming from a momentum-dependent superconducting self-energy. As a result, the feedback effect on spins is present, and one has to solve a set of coupled integral equations for the fermionic propagator and the spin polarization operator. This is the key intent of the present work. We however will not attempt to self-consistently find also the pairing susceptibility which in the spin-fermion model results from multiple spin-fluctuation exchanges in the particle-particle channel [12]. Instead, we assume that below T_c the pairing susceptibility is a conventional δ-function of a total momentum and frequency of a pair with the $d-$wave amplitude Δ_k^2. In other words, we will not distinguish between the true superconducting gap and the pseudogap. The full consideration should indeed include pairing fluctuations into the self-consistent procedure. We will also assume that the fermionic and bosonic self-energies are dominated by the regions near hot spots where $\Delta_k \approx \Delta$ i.e., will neglect the processes which scatter fermions near $(0,\pi)$ into fermions with momenta along zone diagonal where the $d-$wave gap is absent. The contributions from these processes soften sharp features associated with the $k-$independent gap, but are likely to be small numerically as they involve high energy spin fluctuations with momenta far from Q. Still, however, we will fully explore the fact that for $d_{x^2-y^2}$ symmetry of the gap, $\Delta_{k+Q} = -\Delta_k$.

We now derive a set of coupled equations for fermionic and spin propagators in a superconducting state. The derivation procedure is conceptually similar to the derivation of the Eliashberg equations for conven-

tional superconductors. We introduce normal and anomalous fermionic Green's functions $G(k,\omega) = G_0(k,\omega)/(1 + \Delta_k^2\ G_0(k,\omega)\ G_0(-k,-\omega))$ and $F(k,\omega) = -i\Delta_k/(1 + \Delta_k^2\ G_0(k,\omega)\ G_0(-k,-\omega))$ where $G_0^{-1}(k,\omega) = \omega - \Sigma_\omega - \mathbf{v}_F(\mathbf{k} - \mathbf{k}_F)$. The fermionic self-energy formally has the same form as in the normal state, but besides new $G(k,\omega)$, it also contains the spin susceptibility $\chi(q,\Omega) = \chi_0\xi^2/(1 + (q-Q)^2\xi^2 - \Pi_\Omega)$ with the fully renormalized Π_Ω. The latter in turn is the convolution of GG and FF which include fermionic self-energy. This procedure yields a set of two coupled integral equations for *complex* variables $\Sigma(\omega)$ and Π_Ω.

$$\begin{aligned}
\Sigma_\omega &= 3ig^2 \int \frac{d^2q d\Omega}{(2\pi)^3}\ G(k+q,\omega+\Omega)\ \chi(q,\Omega) \\
\Pi_\Omega &= -16i\bar{g}\xi^2 \int \frac{d^2k d\omega}{(2\pi)^3}\ (G(k,\omega)\ G(k+Q,\omega+\Omega) \\
&\quad + F(k,\omega)\ F(k+Q,\omega)) \qquad (2)
\end{aligned}$$

It is instructive to consider first the solution of Eqs (2) in the weak coupling limit $\Delta \ll \bar{g} \ll v_F\xi^{-1}$. To first approximation, Π_Ω can then be evaluated with the free fermion Green's functions. This has been done before [13] and we just quote the result: in the superconducting state, Π_Ω has both real and imaginary parts. The $Im\Pi_\Omega = 0$ for $\Omega < 2\Delta$, it jumps at $\Omega = 2\Delta$ to $\pi\Delta/\omega_{sf}$, and then increases and approaches Ω/ω_{sf} at $\Omega \gg 2\Delta$. This behavior is similar to that in an $s-$wave superconductor except for the jump which is absent in $s-$wave case and is directly related to the fact that $\Delta_{k+Q} = -\Delta_k$.

The $Re\Pi_\Omega$ can be obtained either directly or using the Kramers-Kronig relation. At $\Omega \ll \Delta$, we have $Re\Pi(\omega) = (\pi/8)\ \Omega^2/(\Delta\omega_{sf})$. It diverges at 2Δ as $\Pi_\Omega = (\Delta/\omega_{sf})\log(2\Delta/|2\Delta - \Omega|)$ because of the jump in $Im\Pi_\Omega$, and decreases at larger frequencies. Due to the divergence, $Re\Pi_\Omega$ reaches 1 at a frequency Ω_{res} which is less than 2Δ, i.e., when $Im\Pi_\Omega$ is still zero. Explicitly, $\Omega_{res} = 2\Delta(1 - Z)$ where $Z \propto e^{-\omega_{sf}/(2\Delta)}$. Near Ω_{res}, $\chi(Q,\Omega) \propto Z/(\Omega - \Omega_{res} - i\delta)$, i.e., the dynamical structure factor has a resonance peak.

Consider next the fermionic spectral function. Without self-energy corrections, $A(k,\omega)$ near a Fermi surface resonates at $\omega_{res} = \Delta$. The self-energy gives rise to a fermionic decay. For $s-$wave superconductor, the onset frequency for a decay is 3Δ, and $Im\Sigma(k,\omega)$ emerges as

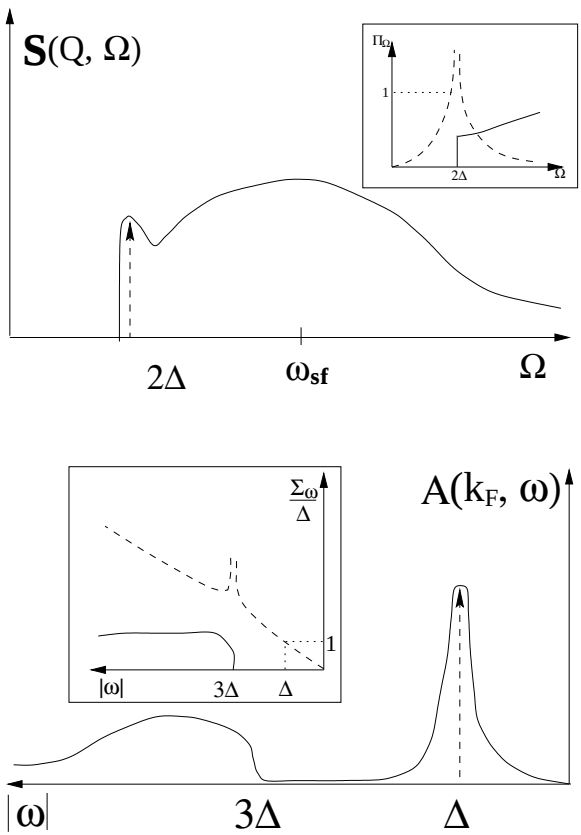

Figure 1: The $T = 0$ weak coupling behavior of the dynamical structure factor and the spectral function. Solid lines are schematic solutions of Eqs. (2) broadened by experimental resolution. Without resolution, the peaks are δ-functions as indicated by arrows. The insets show the spin polarization operator Π_Ω and the fermionic self-energy Σ_ω (solid lines – imaginary parts, dashed lines – real parts). The vertical dashed lines denote logarithmical singularities.

$(\omega - 3\Delta)^{1/2}$ [6]. The presence of the resonance mode in a $d-$wave case, qualitatively changes this picture because a fermion can decay into this mode starting from $\omega_0 < 3\Delta$. A simple power counting shows that this process yields a finite jump of $Im\Sigma_\omega$ at the onset frequency and hence the logarithmical singularity in $Re\Sigma_\omega$. The latter in turn increases the self-energy at $\omega \sim \Delta$ and shifts downwards ω_{res} (which is the measured gap), and the onset frequency for $Im\Pi_\Omega$ which, as one can easily demonstrate, exactly equals $2\omega_{res}$. The amounts of the shifts and the amplitude of the jump in $Im\Sigma_\omega$ can be obtained explicitly from Eqs. (2). We found $\omega_0 = 3\Delta(1-\epsilon)$, $\omega_{res} = \Delta(1-\epsilon)$, and $\delta(Im\Sigma_{\omega_0}) = (\pi\Delta/\log 2)\ \epsilon$, where $\epsilon = (3\log 2\sqrt{N}/(64\sqrt{\pi})\ (\bar{g}/\Delta)^{1/2}\ e^{-\omega_{sf}/(2\Delta)}$.

We see that the $d-$wave form of the gap yields qualitative changes in the system behavior compared to the $s-$wave case, (i.e., the reduction of ω_{res} and the onset frequencies for fermionic and bosonic damping), but at $\Delta \ll \omega_{sf}$, these changes are exponentially small and can hardly be measured. In particular, the resonance peak in $S(Q,\omega)$ should be smeared out already by a small experimental resolution. The weak coupling results are shown in Fig 1.

We now turn to strong coupling limit $\bar{g} \gg \Delta \gg (\omega_{sf}\ \bar{g})^{1/2}$. A conventional wisdom would be that the small effects found at weak coupling progressively grow and eventually become dominant in the strong coupling regime. In our case, this would imply that the resonance frequency in $\chi(Q,\Omega)$ goes down from nearly 2Δ to a $\Omega_{res} \propto (\omega_{sf}\ \Delta)^{1/2}$, and that both the deviation of ω_0 down from 3Δ and the jump in $(Im\Sigma_{\omega_0})$ keep increasing with the coupling. We however found that this is not the case, and the evolution of the jump in $(Im\Sigma_{\omega_0})$ is non-monotonic: with increasing coupling, it first increases, then passes through a maximum and decreases. The point is that if the jump in $(Im\Sigma_{\omega_0})$ tends to a nonzero value at $\xi = \infty$, then $Re\Sigma_\omega$ diverges logarithmically at this point, and this pushes down the quasiparticle peak frequency ω_{res} $(\omega_{res} + Re\Sigma_{\omega_{res}} = \Delta)$. One can easily demonstrate that this effect would yield vanishing ω_{res} at $\xi = \infty$, i.e., a gapless superconductivity. However, our analysis of the coupled equations for the fermionic self-energy and spin polarization operator (see below) shows that the system finds a way to preserve a nonzero ω_{res} even at $\xi = \infty$. It does this by eliminating at $\xi = \infty$ the jumps in both $Im\Sigma_\omega$ and $Im\Pi_\Omega$ at the threshold frequencies

for fermionic and bosonic decays. In the absence of the jumps, $Re\Sigma_\omega$ does not diverge at the threshold frequency, and the system can preserve a nonzero ω_{res}.

We now turn to calculations. At strong coupling, one can neglect ω compared to Σ_ω in $G_0(k,\omega)$. Using this and integrating partly over momentum in (2) we obtained

$$\Sigma_\omega = \frac{3R}{8\pi^2} \int \frac{\Sigma_{\omega+\Omega}}{q_x^2 + \Sigma_{\omega+\Omega}^2 - \Delta^2} \frac{d\Omega dq_x}{\sqrt{q_x^2 + 1 - \Pi_\Omega}} \tag{3}$$

$$\Pi_\Omega = \frac{i}{2} \int \frac{d\omega}{\omega_{sf}} \left(\frac{\Sigma_{\Omega-\omega}\ \Sigma_\omega + \Delta^2}{\sqrt{\Sigma_{\Omega-\omega}^2 - \Delta^2}\ \sqrt{\Sigma_\omega^2 - \Delta^2}} + 1 \right) \tag{4}$$

We then solved Eqs. (3) and (4) in a self-consistent manner. Namely, we first obtained regular terms in $Re\Sigma$ and $Re\Pi$ by expanding (3, 4) in the external frequencies. This yields $Re\Sigma_\omega \propto \omega(\bar{g}/\bar{\Delta})^{1/2}$ and $Re\Pi_\Omega \propto \Omega^2/(\bar{\Delta}\omega_{sf})$. In both cases, the frequency integrals are confined to frequencies $\sim \bar{\Delta}$ where the system interpolates between normal state and superconducting behavior, and for estimates, one can use in the integrands the known normal state results for Σ_ω and Π_ω. We then assumed that at some finite frequency ω_0 $Im\Sigma_\omega$ jumps from 0 to some finite value, considered the onset frequency and the amount of the jump as input parameters, and used Kramers-Kronig relation to calculate the logarithmically singular term in $Re\Sigma_\omega$. Adding it to a regular $Re\Sigma_\omega \propto \omega$, we find ω_{res} where $\omega + Re\Sigma_{\omega_{res}} = \Delta$. Substituting next $Re\Sigma_\omega$ into (4) and using the spectral representation for $Im\Pi_\Omega$, we find the threshold frequency for $Im\Pi_\Omega$ at $2\Omega_{res}$ and the amount of the jump at the threshold. We then again use Kramers-Kronig relation to calculate a logarithmically singular contribution to $Re\Pi$, add it to a regular $Re\Pi_\Omega \propto \Omega^2$, and substitute the result into (3) for Σ_ω. Using again the spectral representation for $Im\Sigma_\omega$, we find two self-consistent equations for threshold frequency ω_0 and for the amount of the jump at the threshold.

Solving these two equations analytically, we found that the peak frequency in $A(k_F,\omega)$ (i.e., the measured gap) is now $\omega_{res} = \bar{\Delta} \sim \Delta^2/\bar{g}$. The nonzero $Im\Pi_\Omega$ and $Im\Sigma_\omega$ appear respectively at $2\bar{\Delta}$ and $\omega_0 = \bar{\Delta}(1+a)$ where $a \propto (\omega_{sf}/\bar{\Delta})^{1/2} \propto \xi^{-1}$. The amounts of jumps in $Im\Pi_\Omega$ and $Im\Sigma_\omega$ both scale as $a^{1/2}$ and disappear at $\xi = \infty$ when $\omega_{sf} = 0$. Above

ω_0, $Im\Sigma_\omega$ first increases as $Im\Sigma_\omega \propto (\omega - \omega_0)^\nu$ where $\nu = \sqrt{3} - 1$, and then recovers the normal state, $\sqrt{\omega}$ behavior. Substituting this Σ into $G(\omega)$, we found that it possesses a peak at ω_{res}, a dip at ω_0 and a hump at $\omega_{hump} = \omega_{res}(1+b)$ where $b \sim (\bar{g}/\bar{\Delta})^{3/(4\nu)}\ R^{1/(2\nu)} \log R \propto \xi^{-1/(2\nu)} \log \xi$. At $\xi = \infty$, peak, dip and hump positions coincide with each other, and the peak/dip/hump structure transforms into the edge singularity: $A(\omega) \propto (\omega - \omega_{res})^{-\nu}$.

Further, the fact that $Im\Pi_\Omega = 0$ up to $2\omega_{res}$ implies, via Kramers-Kronig relation, that at small frequencies $Re\Pi_\Omega \propto \Omega^2/(\omega_{sf}\bar{\Delta})$. Substituting this result into $S(q,\omega)$, we find that it possesses a resonance peak at $\Omega_{res} \sim (\omega_{sf}\bar{\Delta})^{1/2} \sim \xi^{-1} \ll 2\bar{\Delta}$. At $q \neq Q$, the peak disperses with q as $\Omega^2 = \omega_{res}^2((1 + ((q-Q)\xi)^2$, until Ω reaches $2\omega_{res}$, and at larger frequencies disappears due to damping.

The strong-coupling behavior of $S(Q,\Omega)$ and $A(k,\omega)$ is presented in Fig. 2. We see that (i) $S(q,\omega)$ possesses a sharp resonance peak at $\Omega_{res} \sim \xi^{-1}$ which shifts with underdoping to lower frequencies, and (ii) $A(k_F,\omega)$ possesses a quasiparticle peak at $\omega = \omega_{res}$, a dip at $\omega_0 = \omega_{res} + \Omega_{res}$, where $Im\Sigma_\omega$ first appears, and a broad maximum at a somewhat higher frequency ω_{hump}. As the momentum moves away from the Fermi surface, the spectral function for frequencies larger than ω_0 disperses with k and recovers the normal state, non-Fermi liquid form with a broad maximum at $\omega \sim \epsilon_k^2/\bar{g}$. The quasiparticle peak however cannot move further than ω_0 because of a strong fermionic damping above the threshold. We found that it pins at ω_0 and just gradually looses its strength with increasing $k - k_F$. We emphasize that although the resonance frequency in $S(Q,\omega)$ continuously evolves from weak to strong coupling, the physics changes qualitatively between the two limits. At weak coupling, the peak is solely due to a jump in $Im\Pi_\Omega$. At strong coupling, the jump is almost gone, and the existence of peak is due to Ω^2 behavior of $Re\Pi_\Omega$ which is related to vanishing $Im\Pi_\Omega$ below $2\omega_{res}$.

We now compare our results with the data. The peak/dip/hump structure of $A(k,\omega)$, the absence of the peak dispersion, and the presence of the dispersing resonance mode in $S(q,\omega)$ all agree with the ARPES and neutron measurements in $YBCO$ and $Bi2212$ [1, 2, 3, 4]. More quantitatively, we predict that the peak-dip separation in $A(k,\omega)$ at a hot spot exactly equals to the resonance frequency in $S(Q,\Omega)$. Experimentally, in

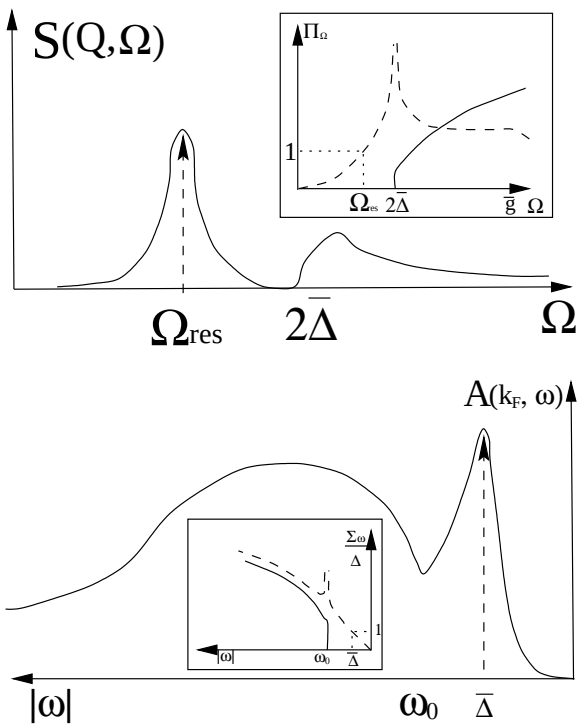

Figure 2: Same as in Fig 1 but at strong coupling. The resonance and onset frequencies are presented in the text. The spin resonance frequency $\Omega_{res} \propto \xi^{-1}$, is equal to the distance between the measured gap $\bar{\Delta}$ and the dip frequency ω_0. The hump frequency differs from $\bar{\Delta}$ roughly by $\xi^{0.7}$.

near optimally doped, $T_c = 87K$ $Bi2212$, $\omega_0 - \omega_{res} \approx 42meV$ [1]. Recent neutron scattering data [4] on $Bi2212$ with nearly the same $T_c = 91K$ yielded $\Omega_{res} = 43meV$, in full agreement with the theory.

We now connect our work to earlier studies. That the interaction with a nearly resonant collective mode peaked at Q explains the ARPES data has been known for some time, and qualitative arguments have been displayed first in [14] and then in [1]. Ref [1] also conjectured that the peak-dip separation may be related to a neutron peak frequency. It has been also realized earlier that in a $d-$ wave superconducting Fermi gas, $S(Q,\Omega)$ contains a resonance peak exponentially close to 2Δ [13]. From this perspective, the key intension of this work was to present the quantitative results for cuprates by performing actual strong coupling calculations, and to explicitly relate ARPES and neutron scattering data.

Morr and Pines [16] obtained the spin-wave like dispersion in $\chi(q,\Omega)$ below T_c by phenomenologically adding the Ω^2 term to the bare susceptibility. This term should be in the form Ω^2/ϵ_F as it can only come from high-energy fermions. We have demonstrated that at $T < T_c$, the system generates an Ω^2/Δ term which for $\Delta \ll \epsilon_F$ completely overshadows a possible bare Ω^2 term.

Morr and one of us [9] considered an approximate solution of Eq. (4) assuming that Π_Ω still has the same purely relaxational form $i\Omega/\omega_{sf}$ as in the normal state, but ω_{sf} is momentum dependent. This approximation does not satisfy the Kramers-Kronig relation, but was argued in [9] to reasonably describe the electronic spectral function at finite temperatures. Comparing our results with [9], we found that the approximate solution captures the peak/dip/hump structure of $A(k,\omega)$, but yields incorrect values of the peak and dip frequencies for $\bar{\Delta} \gg \omega_{sf}$.

J. Brinckman and P. Lee studied the evolution of the resonance peak within the slave boson theory [17]. Their philosophy and the results are similar to ours.

Another interpretation of the neutron experiments was proposed by Zhang and Demler [18, 19]. They attributed the neutron peak to the antibound state at $q = Q$ in the d-wave, spin-triplet particle-particle channel (the π channel). In a $d-$wave superconductor, this channel is coupled to a particle-hole channel (probed by a spin susceptibility) via anomalous Green functions. We performed the same calculations as they

did and at strong coupling *did not* find a sharp antibound state because of strong fermionic incoherence which extends the particle-hole continuum to higher energies. At weak coupling, the antibound state does exist, but for a Fermi surface with hot spots, we found that its energy is larger than $\bar{g} + 2\Delta$, i.e., it *cannot* be located below the threshold frequency for spin damping. We therefore found no evidence for the antibound state at low frequencies. We also reproduced for the model of Eq. (1) the result of Ref [17] that in a $d-$wave superconductor, the $< \pi^{\dagger}, \pi >$ correlator is just proportional to the spin susceptibility such that the poles in this correlator simply mimic the poles in $S(Q, \Omega)$.

Finally, contrary to the assertion in [19], we found that the spin-fluctuation model, the extra spectral weight in $S(Q, \Omega)$ in a superconductor, associated with the resonance peak at low frequencies, is compensated only at energies $\sim \bar{g}$ which are parametrically larger than $\bar{\Delta}$. This implies that the typical momenta at which the compensation occurs are far from Q. As a result, the momentum/frequency integrated difference in the spectral weight of $S(q, \Omega)$ between the normal and the superconducting states, weighted with the magnetic factor $\cos q_x + \cos q_y$, is *finite*: $\int d\omega d^2q (cosq_x + cosq_y)\ (S_n(q, \Omega) - S_{sc}(q, \Omega)) \propto \chi_0 \bar{\Delta}$ [20]. Scalapino and White [21] related this integral to the condensation energy of a superconductor.

To summarize, we considered the superconducting phase of cuprates and demonstrated that the resonance peak in the dynamic structure factor and the peak/dip/hump structure of the electronic spectral function near $(0, \pi)$ can simultaneously be explained by a strong spin-fermion interaction and feedback effects in a $d-$wave superconductor. The peak-dip separation at a hot spot exactly equals to the resonance neutron frequency and vanishes at $\xi = \infty$.

A final note. In the discussion above we assumed that Δ is independent on frequency and spin correlation length. In other words, we do not distinguish between the real gap and the pseudogap. In underdoped cuprates, the pairing susceptibility most likely cannot be approximated by a δ function, and has to include the pairing fluctuations into the self-consistent procedure. This problem is currently under study. We did find, however, [15] that underdoped cuprates possess two "gaps": the actual gap $\bar{\Delta}_0 \propto T_c \leq \omega_{sf}$ which progressively goes down with under-

doping, and the pseudogap $\bar{\Delta} \propto v_F^2/\bar{g}$ which increases with underdoping towards the value comparable to a magnetic J, and is the one measured in tunneling and ARPES experiments. Below $\bar{\Delta}_0$, the system behaves as a conventional superconductor, i.e., both fermions and spin fluctuations are undamped at $T = 0$. At intermediate frequencies, $\bar{\Delta}_0 \ll \omega \ll \bar{\Delta}$, the damping is present, but the fermionic density of states and to a lesser extent spin damping are reduced compared to the normal state values. Finally, above $\bar{\Delta}$, the system recovers a conventional normal state behavior.

In this situation, the peak in $S(Q, \Omega)$ at $T \ll T_c$ splits into a truly resonance peak below $2\bar{\Delta}_0$, and a maximum which in weakly underdoped cuprates still has a form of a nearly resonance peak, but with underdoping progressively evolves (with increasing spin damping) into a normal-state relaxational maximum at ω_{sf}. As $\bar{\Delta}_0 \leq \omega_{sf}$, the resonance peak is described by a weak-coupling theory and has a very small residue. In practice, it should appear only as a shoulder-like feature in $S(Q, \omega)$. Above T_c, the shoulder-like feature disappears, but the maximum at Ω_{res} survives up to a temperature which increases with underdoping.

Under the same conditions, the spectral function $A(k, \omega)$ at $T \ll T_c$ should also display two features, the reduction of the spectral weight at frequencies below $\bar{\Delta}$ (the leading edge gap), and a truly quasiparticle peak at $\omega = \bar{\Delta}_0$. The latter, however, has a small residue $\sim 1/R$, and is hardly observable because of resolution. Above T_c, a sharp peak (and hence a dip) disappear, but the leading edge gap should survive by the same reasons as the maximum in $S(Q, \Omega)$. In strongly underdoped cuprates, the reduction of the fermionic density of states below $\bar{\Delta}$ is likely to be rather gradual in which case the leading edge gap transforms into a broad maximum at $\omega \sim \bar{\Delta} \sim J$. This evolution of the behavior of $S(Q, \Omega)$ and $A(k, \omega)$ is fully consistent with the data [1, 2, 3]. We however emphasize that we do not have at the moment a full quantitative description of underdoped systems.

It is our pleasure to thank G. Blumberg, A. Finkelstein, R. Joynt, G. Kotliar, A. Millis, D. Morr, M. Norman, D. Pines and J. Schmalian for useful conversations. The research was supported by NSF DMR-9629839.

References

[1] M. R. Norman *et al.*, Phys. Rev. Lett. **79**, 3506 (1997). M.R. Norman and H. Ding, Phys. Rev. B **57** R11089 (1998).

[2] Z-X. Shen et al, Science **280**, 259 (1998).

[3] H.F. Fong et al, Phys. Rev. B **54**, 6708 (1996); P. Dai et al, Science **284**, 1344 (1999).

[4] H.F. Fong et al, Nature **398**, 588 (1999).

[5] Ch. Renner *et al.*, Phys. Rev. Lett. **80**, 149 (199).

[6] D. Coffey, Phys. Rev. B **42**, 6040 (1990); P.B. Littlewood and C.M. Varma, Phys. Rev. B **46**, 405 (1992).

[7] G. Blumberg et al , A. Chubukov and D. Morr, Solid State Comm, to appear.

[8] A. Chubukov, Europhys. Lett. **44**, 655 (1997).

[9] A. Chubukov and D. Morr, Phys. Rev. Lett. **81**, 4716 (1998).

[10] A. Georges et al, Rev. Mod. Phys., **68**, 13 (1996).

[11] L. Kadanoff, Phys. Rev. **132**, 2073 (1963).

[12] P. Monthoux and D. Pines, Phys. Rev. B **47**, 6069 (1993) D.J. Scalapino, Phys. Rep. **250**, 329 (1995).

[13] D.Z. Liu, Y. Zha and K. Levin, Phys. Rev. Lett. **75**, 4130 (1995); I. Mazin and V. Yakovenko, ibid **75**, 4134 (1995); (1991); A. Millis and H. Monien, Phys. Rev. B **54**, 16172 (1996); N. Bulut and D. Scalapino, Phys. Rev. B **53**, 5149 (1996).

[14] Z-X. Shen and J.R. Schrieffer, Phys. Rev. Lett. **78**, 1771 (1997).

[15] A. Abanov, A. Chubukov and A. Finkelstein, in preparation.

[16] D.K. Morr and D. Pines, Phys. Rev. Lett. **81**, 1086 (1998).

[17] J. Brinckmann and P.A. Lee, Phys. Rev. Lett. **82**, 2915 (1999).

[18] E. Demler and S.-C. Zhang, Phys. Rev. Lett. **76**, 4126 (1995).

[19] E. Demler and S.-C. Zhang, Nature **396**, 733 (1998).

[20] A. Abanov and A. Chubukov, in preparation.

[21] D. Scalapino and S. White, Phys. Rev. B **58**, 8222 (1998).

Magnetism of Nanostructured Systems

Yu.G. Pogorelov

CFP/IFIMUP, Departamento de Física, Universidade do Porto, Portugal

I.- What are nanostructured systems (NSS) and why are they of interest?

These are the artificially prepared composite materials with strong modulation of physical parameters (electronic, magnetic, etc.) on nm-scale d (supposing $a < d < l$, where a is the atomic size and l the characteristic correlation length in solid).

What particular kinds of NSS are addressed here:

composition structure	M-metal/NM-metal	M-metal/insulator
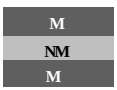 sandwiched	Spin-valves (SV) B. Dieny et al (1991)[1]	Spin-tunnel junctions (STJ) J. Moodera et al (1995)[2]
 multilayered (superlattices)	GMR multilayers (M. Baibich et al, 1988)[3]	
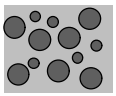 3D granular	CoAg, CoCu, etc. alloys A. Berkowitz et al, 1992)[4]	Cermets NiFe/SiO_2, Co/Al_2O_3 Gittleman et al, 1972)[5]
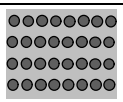 discontinuous multilayers		DMIM's B. Dieny et al, 1997)[6] DTJ's S. Sankar et al, 1998)[7]

Not considered are: hybride magnetic-semiconductor systems, metallic nanowires, magnetic quantum dots, ferrofluids, …

Why are NSS of interest?

Combination of electronic parameters (metallic: Fermi density of states n_F, Fermi momentum k_F, mean free path l, and spin-flip mean free path $l_{s\text{-}cf}$,… and insulating: tunnel barrier height W, dielectric constant e ,…), magnetic parameters (saturation magnetization M_s, anisotropy K_a, coercive field H_c,…), and structural parameters (thickness t and number n of magnetic layers, spacer thickness s, granule size d and concentration x, intra-layer and inter-layer spacings,…) makes them perhaps the most versatile class of materials.

From the fundamental point of view, NSS are the systems which properties are essentially influenced by *correlations* between nanocomponents, and these correlations can be *controlled* either by preparation techniques or by external parameters. This permits one to tailor new properties of the composite, not existing in each separate component.

II.- Principal phenomenology of NSS

- Oscillating magnetic coupling between magnetic layers, with complex periodicity in either t and s (S. Parkin et al;[8] P. Bruno[9]).
- Giant magnetoresistance (GMR) in multilayered structures (M. Baibich et al, 1988). It can be realized in two different experimental geometries: current-in-plane (CIP) and current-perpendicular-to-plane (CPP) (Fig. 1).

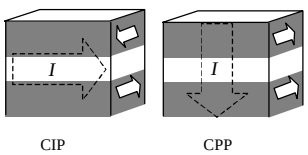

Fig. 1

- Oscillatory dependence of GMR on spacer thickness s (Mosca et al[10]).
- GMR in granular materials (Gittleman et al, 1972; Berkowitz et al, 1992; Xiao et al,[11]).
- GMR, correlated with magnetization processes in SV's (B. Dieny et al, 1991), in STJ's (J. Moodera et al, 1995), and in DMIM's (B. Dieny et al, 1997).

All these phenomena evidence considerable magnetic correlations between nanocomponents. Their understanding is based on several assumptions:

- Each magnetic component is considered as a saturated (by strong internal exchange), single-domain ferromagnet.
- Much weaker (but long-ranged) interaction between components is due to:
  a) effect by conduction electrons (mostly in metals),
  b) dipolar interactions (always)
- Relation between magnetic correlations and magnetotransport properties is realized through:
  a) spin-dependent scattering (in M-M systems),
  b) spin-dependent tunneling (in M-I systems).

III.-How indirect magnetic coupling is realized in different NSS?

A consistent analysis of this mechanism for multilayered systems was developed by P. Bruno,[9] using the idea of quantum interference for conduction electrons of each spin polarization and subsequent modification of their density of states $n(e)$ and of full electronic energy E. Thus, for the simplest configuration of 1D potential well (Fig. 2) characterized by the reflection coefficients $r_A = |r_A|e^{i\varphi_A}$ and $r_B = |r_B|e^{i\varphi_B}$ for an electron with momentum k, interference is constructive (destructive) when the phase shift after round trip:

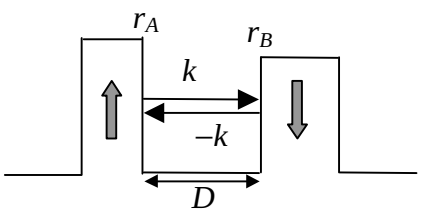

Fig. 2

$\Delta\varphi = 2kD + \varphi_A + \varphi_B$, is p times even (odd) number. The related change in the density of states $\Delta n(\varepsilon) \approx (2/\pi) Im[2iD(dk/d\varepsilon) r_A r_B e^{2ikD}]$ results in the change of total energy:

$$\Delta E = \frac{2}{\pi} Im \int_{-\infty}^{\varepsilon_F} \ln(1 - r_A r_B e^{2ikD}) d\varepsilon$$

At least, the spin dependence of $r_{A,B} \to r_{A,B}^{\uparrow,\downarrow}$ defines the coupling energy between layers (at $T = 0$):

$$J = \Delta E_F - \Delta E_{AF} = \frac{1}{4\pi^3} \int d^2k_7 \int_0^{\varepsilon_F} \ln \frac{(1 - r_A^{\uparrow} r_B^{\uparrow} e^{2ikD})(1 - r_A^{\downarrow} r_B^{\downarrow} e^{2ikD})}{(1 - r_A^{\uparrow} r_B^{\downarrow} e^{2ikD})(1 - r_A^{\downarrow} r_B^{\uparrow} e^{2ikD})} d\varepsilon$$

which oscillates in function of D

In a similar way, the indirect coupling between magnetic granules in a granular alloy can be obtained from consideration of a spin-dependent scattering operator:[12]

$$\hat{W}(r) = \sum_{\alpha} \chi_{\alpha}(\boldsymbol{r})(U + I\hat{\sigma} \cdot \boldsymbol{m}_{\alpha}) \qquad (1)$$

where $c_a(\boldsymbol{r})$ is 1 within a-th granule (magnetized along unit vector $\boldsymbol{m}_a$) and 0 otherwise, $\hat{\sigma}$ is electronic spin. The corresponding Born amplitude:

$$\hat{w}(q) = \int e^{iqr} \hat{W}(r) dr \qquad (2)$$

$\boldsymbol{q}$ being the momentum transfer (Fig. 3), gives rise to the energy change:[13]

$$\Delta E = \sum_{k,\, q} \frac{n_k(1 - n_{k+q})}{\varepsilon_k - \varepsilon_{k+q}} Tr\hat{w}(q)\hat{w}(-q) = -\frac{I^2}{\varepsilon_{F\alpha,}} \sum_{\alpha' \neq \alpha} m_{\alpha} \cdot m_{\alpha'} F(r_{\alpha\alpha'}) + spin\ indep$$

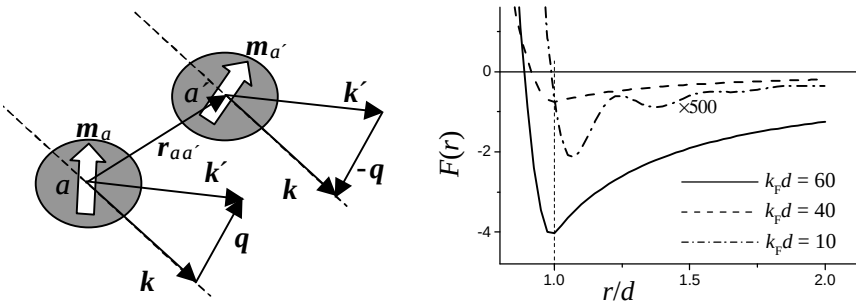

Fig. 3

The dimensionless function $F(r)$ was calculated for identical spherical granules of diameter d (Fig. 3), it describes almost monotonic decrease of AFM coupling (some remnants of RKKY-like oscillations are seen for smaller values of $k_F d$). The maximum overall effect of such coupling in a uniformly magnetized sample results in a certain demagnetizing field (besides the common dipolar field) $H_{dem,\, el} \sim 0.01\, fI^2/(e_F m_B)$, where f is the granule filling factor.

IV.-Magnetic correlations and GMR in NSS

Negative magnetoresistance in NSS is due to less spin-dependent scattering (or easier spin-dependent tunneling) at alignment of magnetic moments of nanocomponents by the applied magnetic field (Fig. 4). Similar effect takes place at suppression of critical fluctuations near T_C in FM metals, but static fluctuations in NSS (with much shorter wavelengths) scatter electrons much stronger, hence the name "giant" for the related field effect.

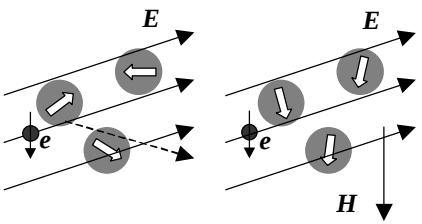

Fig. 4

The simplest idea of GMR in CIP geometry in multilayered systems is illustrated by the equivalent circuit model. The magnetoresistance coefficient $\Delta R/R = R_F/R_{AF} - 1$ results negative since

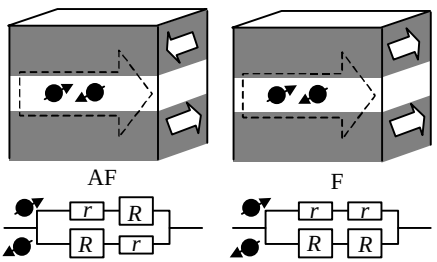

Fig. 5

$$R_{AF} = \frac{r+R}{2} = \bar{r} > R_F = \bar{r} - \frac{\Delta^2}{\bar{r}}$$

where $\Delta = (R - r)/2 \sim m$ (the magnetization), and equals: $\frac{\Delta R}{R} = -\frac{\Delta^2}{\bar{r}^2} \sim -m^2$

The proportionality $-\Delta R/R \sim m^2$ is often observed in experiment, however some deviations from it also occur, especially at low m,[4] indicating that MR is sensitive not only to uniform magnetic order

A number of successful theories was elaborated for GMR in multilayers. The classical approach of Boltzmann equation is controlled by the boundary conditions at interfaces through spin-dependent reflection and transmission coefficients and diffuse scattering for CIP geometry,[14] and through spin accumulation potentials for CPP geometry.[15] Further, the quantum treatment within Kubo formalism was also developed for multilayered[16] and spin-valve[17] structures. This progress was generally determined by a well defined spatial periodicity of such systems. However the situation for granular systems is not so clear and needs a special care.

S. Zhang and P. Levy extended their description of CPP GMR (Ref. 16) to granular films,[18] using the Drude formula

$$\sigma = \frac{ne^2}{2m}\sum_{\sigma}\frac{1}{\Delta^{\sigma}} \tag{3}$$

with spin-dependent imaginary parts of self-energy:

$$\Delta^2 = \pi\sum_{k'}\left|V^{\sigma}_{kk'}\right|^2\delta(\varepsilon_k - \varepsilon_{k'}) \tag{4}$$

The scattering potential they used:

$$V(r,\hat{\sigma}) = \sum V_j^{(nm)}\delta(r - r_j) + \sum_{\alpha}\sum_{j\in\alpha} V_j^{(m)}(1 + p_b\hat{\sigma}\cdot\hat{S}_j)\delta(r - r_j^{\alpha})$$
$$+ \sum_{\alpha}\sum_{s\in\alpha} V^{(s)}(1 + p_s\hat{\sigma}\cdot\hat{S}_s)\delta(r - r_s^{\alpha})$$

with (*nm*, *m*, *s*) related to non-magnetic, magnetic, and interface atoms, couples $\hat{\sigma}$ to spin operators $\hat{S}_j$ of *j*-th atom within a-th granule (substituted simply by their mean values $\boldsymbol{m}_a$ in $\hat{W}(r)$, Eq. (1)). The calculation of Δ^s, Eq. (4), restricted only to diagonal terms in a,j (single-site processes), yields in

$$\frac{\Delta R}{R} = \left(\frac{\xi_1}{\xi_0}\right)^2 \text{ with}$$

$$\xi_1 = 2f'[p_b\lambda_m^{-1}\overline{m(\nu)} + p_s\lambda_s^{-1}\overline{m(\nu)\nu^{-1/3}}]$$
$$\xi_0 = (1-f)\lambda_{nm}^{-1} + f[(1+p_b^2)\lambda_m^{-1} + (1+p_s^2)\lambda_s^{-1}\overline{\nu^{-1/3}}],\ \lambda_k^{-1} \sim \left|V^{(k)}\right|^2$$

, that is $\Delta R/R \sim m^2$.

However, the important dependence on short-range magnetic order $\langle\cos q_{12}\rangle = \langle \boldsymbol{m}_a\cdot\boldsymbol{m}_{a'}\rangle$ should come from non-diagonal terms in a,a' (mainly between nearest neighbor granules). To take this account, write the Drude formula, Eq. (2), as:[12]

$$\sigma = \frac{ne^2}{2m}Tr\hat{\tau} \tag{5}$$

where the inverse of matrix $\hat{\tau}$:

$$\hat{\tau}^{-1} = \frac{\pi n_F}{2\hbar k_F^4}\int_0^{2k_F} q^3|\hat{w}(q)|^2 dq$$

resembles common inverse relaxation time,[19] but includes the spin-dependent amplitudes, Eq. (2). The resulting expression for MR:

$$-\frac{\Delta R}{R} = \frac{f^2\Gamma I^2}{D(f)}\left[\beta\langle\cos\theta_{12}\rangle + \frac{\Gamma[2U(\alpha\ln k_F d - f\beta)]^2}{D(f) - f\beta\langle\cos\theta_{12}\rangle I^2}m^2\right] \qquad (6)$$

where $D(f) = t_0^{-1}k_F d + f\Gamma[a(U^2 + I^2)\ln 2k_F d - fbU^2]$, t_0 is the relaxation time not related to granules, $\Gamma = 6n_F/\hbar$, $a \approx 4.83$, $b \approx 17.53$, displays the short-range order contribution $\sim \langle\cos q_{12}\rangle$ which can be comparable or even greater than the long-range order contribution $\sim m^2$ in the "dirty" limit $D \approx t_0^{-1}k_F d$. A characteristic crossover from quadratic to linear $\Delta R/R(f)$ dependence at passing to "clean" limit $D(f) \propto f$ in Eq. (6) is well confirmed by the experimental data.[20-22] Another interesting feature is the field dependence $\Delta R/R(H)$, revealing a non-monotonous behavior if the distribution of granule sizes is "bimodal" with $d_1 < d_2$ (Fig. 6). Here three characteristic regions correspond to consecutive saturation of correlations between two great (g-g), small and great (g-s), and two small (s-s) granules[23] in good agreement with prediction by Eq. (6).

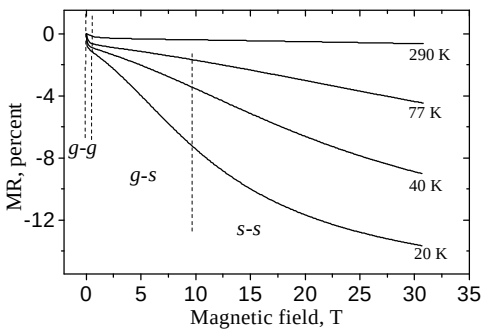

Fig. 6

V.- Tunnel magnetoresistance (TMR) in metal-insulator NSS

Enhanced magnetoresistance in STJ's is understood within the concept of spin-dependent Fermi densities of states $n_F{}^s$, defining the balance of tunneling rates for spin polarized electrons through the tunnel barrier (Fig. 7).[24,25] The junction conductance $G = (e^2/h)|T|^2$ is controlled by the transmission probability $|T|^2 \propto (1 + P^2\cos q)e^{-2cs}$ where $c = (2mj/\hbar)^{-1/2}$, $P = (n_F{}^{\uparrow} - n_F{}^{\downarrow}) / (n_F{}^{\uparrow} + n_F{}^{\downarrow})$ is the polarization of each electrode, and q the relative angle between magnetizations of electrodes. Hence the maximum MR is (ΔR/

$R)_{max} = 1 - G_{AF}/G_F = -2P^2/(1 + P^2)$. This formula was extended by J. Inoue and S. Maekawa for cermet thin films to give:[26]

$$\frac{\Delta R}{R} = \frac{P \langle \cos\theta \rangle}{1 + P \langle \cos\theta \rangle} \qquad (7)$$

averaged over orientations of neighbor granule moments. Thus TMR is fully determined by the short-range correlations as was suggested long ago.[5]

At passing to discontinuous multilayered systems one have also to consider a strong difference of magnetic correlations between granules within the same layer and between granules in adjacent layers, leading to dissimilarities between CIP and CPP TMR. For CIP conductance, the average $\langle \rangle_\perp$ is mainly taken over the in-series tunnel resistances within the layer, when CPP relates to the average $\langle \rangle_z$ for parallel tunnel conductances across layers. The respective TMR expressions are different:[27]

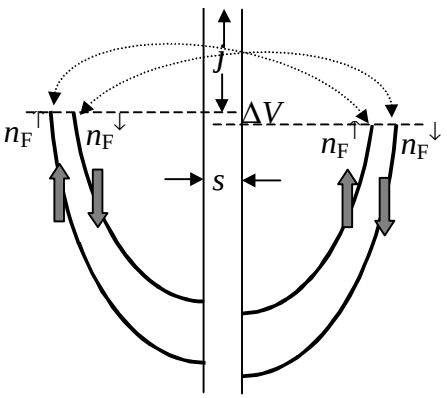

Fig. 7

$$\frac{\Delta R}{R}_{CIP} = \frac{P\ (1 - \langle \cos\theta \rangle_\perp)}{1 + P \langle \cos\theta \rangle_\perp} \qquad \frac{\Delta R}{R}_{CPP} = \frac{P\ (1 - \langle \cos\theta \rangle_z)}{1 + P} \qquad (8)$$

and, correspondingly, a substantial difference was observed between the temperature behavior of $(\Delta R/R)_{CIP}$ (a strong increase at low T) and $(\Delta R/R)_{CPP}$ (almost T-independent).

VI.-Mean-field model for dipolar correlations in granular magnetic systems

The simplest approach to magnetization M of an ensemble of superparamagnetic particles through averaging of Langevin function $L(M_S vH/T)$, $L(x) = \coth x - 1/x$, over granule volumes v with certain distribution $P(v)$ leads to a universal dependence $M = M(H/T)$ on the ratio H/T, not on H and T separately. But this universality not always holds, even in rather diluted systems. Besides the effects of uniaxial anisotropy (accounted for in the Stoner-Wohl-

fahrt model[28]), also the long-ranged dipolar interactions between granules can modify essentially free energy F and related magnetic properties of a granular system. The mean-field analysis of F dependence on granule size, shape, and concentration[29,30,13] yielded in the expression:

$$F = -f\boldsymbol{M}\boldsymbol{H} + \frac{1}{2}f\boldsymbol{M}[(1-f)\hat{N}_g + f\hat{N}]\boldsymbol{M} \qquad (9)$$

where the demagnetizing tensors and are related to the whole sample and to a granule. Then considering the Langevin functions $L(M_s v H_i/T)$ with the internal field on granule: $\boldsymbol{H}_i = \boldsymbol{H} - [(1 - f) + f]\boldsymbol{M}$, leads to a self-consistent equation, which for spherical granules and external field $\boldsymbol{H}$ in the plane of a thin film sample reads:

$$H_i = H + -\frac{4\pi}{3}\frac{1-f}{f}M_s\int_0^\infty P(\nu)L\left(\frac{M_s \nu H_i}{T}\right)d\nu \qquad (10)$$

A simple solution for static magnetic susceptibility: $c^{-1} = c_0^{-1} + T/C$ with $c_0^{-1} = 4p(1-f)/(3f)$, $C = fM_s^2/3$, and $= f^{-1}\int vP(v)dv$, demonstrates deviation from the genuine Langevin behavior $c^{-1} \propto T$, in an agreement with the measurements for $Co_{1-x}Ag_x$ granular films.[5]

With growing concentration f, granules tend to merge into warm-like structures (Fig. 8), and above some critical value f_p, referred to as magnetic percolation point (which can be well below true structural percolation),[31] a finite fraction f_{FM} of the composite behaves as FM continuum whereas the resting "granular" fraction $f_g = f - f_{\mathrm{FM}}$ stays sensitive to granule shape and size. Then Eq. (9) transforms into:

Fig. 8

$$F = -(f_g\boldsymbol{M}_g + f_{FM}\boldsymbol{M}_{FM})\boldsymbol{H} \qquad (11)$$
$$+\frac{1}{2}[f_g(1-f_g)\boldsymbol{M}_g\hat{N}_g\boldsymbol{M}_g + (f_g\boldsymbol{M}_g + f_{FM}\boldsymbol{M}_{FM})\hat{N}(f_g\boldsymbol{M}_g + f_{FM}\boldsymbol{M}_{FM})]$$

and the internal fields on each fraction are different, $\boldsymbol{H}_{i\mathrm{FM}} = \boldsymbol{H} - \hat{N}(f_g\boldsymbol{M}_g + f_{\mathrm{FM}}\boldsymbol{M}_{\mathrm{FM}})$ and $\boldsymbol{H}_{ig} = \boldsymbol{H} - (1-f_g)\hat{N}_g\boldsymbol{M}_g - \hat{N}(f_g\boldsymbol{M}_g + f_{\mathrm{FM}}\boldsymbol{M}_{\mathrm{FM}})$. This leads to an interesting effect on dynamic magnetic susceptibility of granular films, probed by ferromagnetic resonance (FMR) from the coupled Landau-Lifshitz equations $\dot{\boldsymbol{M}}_g = -\gamma\boldsymbol{M}_g \times \boldsymbol{H}_{ig}$, and $\dot{\boldsymbol{M}}_{FM} = -\gamma\boldsymbol{M}_{FM} \times \boldsymbol{H}_{iFM}$. They give rise, in gen-

eral, to two different resonance fields at varying the angle q_H between $\boldsymbol{H}$ and the normal to film.[31] This predicted splitting was recently observed in $Co_{1-x}Ag_x$ granular films (Fig. 9).[32]

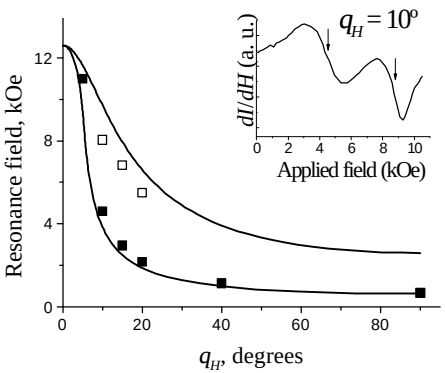

Fig. 9

VII.-Conclusions

Above brief survey of different electronic, magnetic, and transport properties of nanostructured systems indicates an essential role of magnetic correlations between nanoparts of such systems and permits to conclude that their novel and unusual macroscopic properties reflect some new fundamental physical processes, characteristic of these artificial materials. Further study in this field, which should go beyond the mean-field models, can bring a deeper insight on the physics of nanomagnetism and yield in new useful applications.

This work was supported by Portuguese Program PRAXIS XXI through research projects 3/3.1/FIS/21/94 and 2/2.1/FIS/302/94 and the grant BPD/14226/97.

VIII.-References

1. B. Dieny, V.S. Speriosu, S.S.P. Parkin, B.A. Gurney, D.R. Wilhoit, and D. Mauri, Phys. Rev. B**43**, 1297 (1991)
2. J.S. Moodera, L.R. Kinder, T.M. Wong, R. Meservey, Phys. Rev. Lett. **74**, 3273 (1995).
3. M.N. Baibich, J.M. Broto, A. Fert, F. Nguen Van Dau, F. Petroff, P. Etienne, G. Greuzet, A. Friederich, and J. Chazelas, Phys. Rev. Lett. **61**, 2472 (1988).
4. A. Berkowitz, J.R. Mitchell, M.J. Carey, A. P. Young, S. Zhang, F.E. Spada, F.T. Parker, A. Hutten and G. Thomas, Phys. Rev. Lett. **68**, 3745 (1992).
5. J.I. Gittleman, Y. Goldstein, and S. Bozowski, Phys. Rev. B**5**, 3609 (1972).

6. B. Dieny, S. Sankar, M.R. McCartney, D.J. Smith, P. Bayle-Guillemaud, A.E. Berkowitz, J. Magn. and Magn. Mat. **185**, 283 (1997).
7. S. Sankar, B. Dieny, A.E. Berkowitz, J. Appl. Phys. **81**, 5512, (1997).
8. S.S.P. Parkin, N. More, and K.P. Roche, Phys. Rev. Lett. **64**, 2304 (1990).
9. P. Bruno, Phys. Rev. B**52**, 411 (1995).
10. D.H. Mosca, F. Petroff, A. Fert, P.A. Schroeder, W.P. Pratt Jr. and R. Laloee, J. Magn. Magn. Mat, **94**, L1 (1991)
11. J.G. Xiao, J.S. Jiang, C.L. Chien, Phys. Rev. Lett. **68**, 3749 (1992).
12. Yu.G. Pogorelov, M.M.P. de Azevedo, and J.B. Sousa, Phys. Rev. B**58**, 458 (1998).
13. Yu.G. Pogorelov, G.N. Kakazei, M.M. Pereira de Azevedo, J.B. Sousa, J. Magn. Magn. Mater. **196-197**, 112-114 (1999).
14. R.E. Camley and J. Barnas, Phys. Rev. Lett. **63**, 664 (1989).
15. T. Valet and A. Fert, Phys. Rev. B **48**, 7099 (1993).
16. P.M. Levy, S. Zhang, and A. Fert, Phys. Rev. Lett. **65**, 1643 (1990).
17. A. Vedyayev, B. Dieny, and N. Ryzhanova, Europhys. Lett. **19**, 329 (1992).
18. S. Zhang and P.M. Levy, J. Appl. Phys, **73**, 5315 (1993).
19. A.A. Abrikosov, Fundamentals of Theory of Metals, North-Holland (1988).
20. C.L. Chien, J.Q. Xiao, J.S. Jiang, J. Appl. Phys. **73**, 5313 (1993).
21. J.-Q. Wang, P. Xiong, G. Xiao, Phys. Rev. B **47**, 8341 (1993).
22. T. Sugawara, K. Takanashi, K. Hono, H. Fujimori, JMMM **159**, 95 (1996).
23. J.B. Sousa, M.M. Pereira de Azevedo, M.S. Rogalski, Yu.G. Pogorelov, L.M. Redondo, C.M. de Jesus, J.G. Marques, M.F. da Silva, J.C. Soares, J.-C. Ousset, E. Snoeck, J. Magn. Magn. Mater. **196-197**, 13-17 (1999).
24. M. Julliere, Phys. Lett. A**54**, 225 (1975).
25. S. Maekawa, U. Gäfvert, IEEE Trans. Magn. **MAG-18**, 707 (1982).
26. J. Inoue and S. Maekawa, Phys. Rev. B**53**, 11927 (1996).
27. G.N. Kakazei, P.P. Freitas, S. Cardoso, A.M.L. Lopes, M.M. Pereira de Azevedo, Yu.G. Pogorelov, J.B. Sousa, IEEE Trans. Magn. (to be published).
28. E.C. Stoner and E.P. Wohlfahrt, Philos. Trans. Roy. Soc. A**240**, 599 (1948).

29. U. Netzelmann, J. Appl. Phys. **68**, 1800 (1990).
30. J. Dubowik, Phys. Rev. B**54**, 1088 (1996).
31. G.N. Kakazei, A.F. Kravets, N.A. Lesnik, M.M. Pereira de Azevedo, Yu.G. Pogorelov, J.B. Sousa, J. Appl. Phys. **85**, 5654-5656 (1999).
32. A.F. Kravets, N.A. Lesnik, G.N. Kakazei, Yu.G. Pogorelov, J.B. Sousa, M.M. Pereira de Azevedo, M. Malinowska, P. Panissod, Phys. Rev. B **60** (1999).

Phase separation and enhanced charge-spin coupling near magnetic transitions

by Daniel P. Arovas[1]*, Guillermo Gómez-Santos*[2] *and Francisco Guinea*[3]

[1] *Department of Physics, University of California at San Diego, La Jolla CA 92093*
[2] *Departamento de Física de la Materia Condensada and Instituto Nicolás Cabrera, Universidad Autónoma de Madrid. Cantoblanco. E-28049 Madrid , Spain*
[3] *Instituto de Ciencia de Materiales, CSIC, Cantoblanco, 28049 Madrid, Spain*

The generic changes of the electronic compressibility in systems that show magnetic instabilities is studied. It is shown that, when going into the ordered phase, the compressibility is reduced by an amount comparable to the its original value, making charge instabilities also possible. We discuss, within this framework, the tendency towards phase separation of the double exchange systems, the pyrochlores, and other magnetic materials.

I.- Introduction

The possibility of phase separation in magnetic systems was first discussed in connexion to the Hubbard model for itinerant ferromagnetism and antiferromagnetism[1]. Recent results suggest that phase separation is also likely in other magnetic materials, such as those in which magnetism is due to double exchange interactions[2, 3, 4, 5, 6, 7]. Spin polarons, which can be viewed as a manifestation of phase separation on a small scale, have been analyzed in relation to the pyrochlores[8]. Finally,

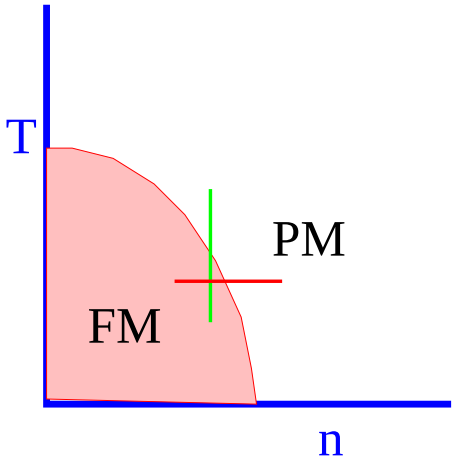

Figure 1: Schematic phase diagram of a magnetic system whose electronic concentration can be continuously varied. The standard Ginzburg-Landau analysis of the transition gives information about the temperature dependence at fixed concentration (vertical line). Phase separation is related to the critical properties *as function of concemtration* (horizontal line).

there is an extensive literature on phase separation in two dimensional doped antiferromagnets (see, for instance[9, 10, 11, 12, 13, 14]), although there is no definitive consensus on its existence. In the following, we outline a general mechanism which support the presence of phase separation near magnetic transitions. A detailed study can be found in[15].

In general, the formation of an ordered phase induces a decrease in the free energy of the material, usually called the condensation energy. Because of it, quantities which depend on the variation of the free energy with temperature, such as the specific heat, show anomalous, non analytic behavior at the critical temperature. For instance, the specific heat shows an abrupt reduction at T_c in mean field theories.

The phase transition can also be tuned by varying the electronic concentration, n, in many systems leading to phase diagrams like that shown in fig.[1]. Thus, one expects an anomalous dependence of the free energy on electronic density as the phase boundary is crossed by changing the electronic concentration.

The electronic compressibility is proportional to the second deriva-

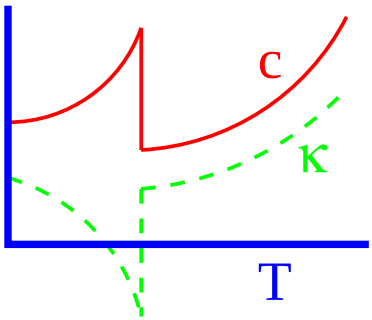

Figure 2: Schematic temperature dependence of the specific heat (full line) and compressibility (broken line) near a magnetic transition.

tive of the free energy with respect to the density. In a related way to the behavior of the specific field, simple arguments show that it should have a discontinuity at the transition, as schematically depicted in fig.[2].

We can get a simple estimate of the effect by using a standard Ginzburg-Landau expansion for the free energy:

$$\begin{aligned} \mathcal{F}(s) &= \frac{c}{2}\int(\nabla s)^2 d^D r + \frac{a[T-T_{\rm c}(n)]}{2}\int s^2 d^D r + \\ &+ \frac{b}{4}\int s^4 d^D r + \mathcal{F}_n(n) \end{aligned} \tag{1}$$

where s is the electronic magnetization and n is the electronic density. We now neglect spatial fluctuations, and obtain a mean field approximation to $\mathcal{F}$:

$$\mathcal{F}_{MF} = \frac{a[T-T_{\rm c}(n)]}{2}s^2 + \frac{b}{4}s^4 + \frac{(n-n_0)^2}{2\kappa} \tag{2}$$

where we have expanded the dependence of the free energy of the paramagnetic phase on n. κ is the electronic compressibility, and n_0 defines the equilibrium density in the absence of magnetism. When $T < T_{\rm c}$, the magnetization is: $s = \frac{a[T_{\rm c}(n)-T]}{b}$ and the free energy becomes:

$$\mathcal{F}_{MF} = -\frac{a^2[T_{\rm c}(n)-T]^2}{4b} + \frac{(n-n_0)^2}{2\kappa} \tag{3}$$

Let us now fix the temperature T and expand this expression around the density n_c such that $T = T_c(n_c)$. We obtain:

$$\mathcal{F}_{MF} \approx -\frac{a^2}{4b}\left(\frac{\partial T_c}{\partial n}\right)^2 (n - n_c)^2 + \frac{(n-n_0)^2}{2\kappa} \tag{4}$$

And by taking derivatives, we have:

$$\frac{\partial^2 \mathcal{F}_{MF}}{\partial n^2} = \begin{cases} \frac{1}{\kappa} & T_c < T \\ -\frac{a^2}{2b}\left(\frac{\partial T_c}{\partial n}\right)^2 + \frac{1}{\kappa} & T < T_c \end{cases} \tag{5}$$

The compressibility has a jump at the transition. The origin of this discontinuity is the same as that in the specific heat. Moreover, it is reasonable to expect that this anomaly will be enhanced when fluctuations in the critical region are taken into account.

Alternatively, and keeping T fixed, one can minimize eq.(2) first with respect to n. By expanding $T_c(n)$ around n_0, we find:

$$n \approx \begin{cases} n_0 & T_c < T \\ n_0 + \frac{a\kappa s^2}{2}\frac{\partial T_c}{\partial n} & T < T_c \end{cases} \tag{6}$$

and, inserting the value of n in the free energy when $T < T_c$:

$$\mathcal{F} \approx \frac{a[T_c(n_0) - T]}{2} s^2 + \frac{b}{4} s^4 - \frac{a^2\kappa}{8}\left(\frac{\partial T_c}{\partial n}\right)^2 s^4 \tag{7}$$

The dependence of T_c on density leads to a negative quartic term in the dependence of the free energy on the magnetization. When $b/4 - (a^2\kappa)(\partial T_c/\partial n)^2/8 < 0$, the magnetic transition becomes first order. This condition is equivalent to saying that the effective compressibility, defined in eq.(5) becomes negative. Thus, phase separation near the transition can be thought of as arising from the transmutation of a continuous phase transition into a first order one by the introduction of an additional field, the density n, which is a well known possibility in statistical mechanics[16]. The new feature found in a magnetic transition is that the correction to the compressibility can easily be comparable to the initial compressibility. The latter is determined by the density of states at the Fermi level in the paramagnetic phase. In typical magnetic systems,

the transition is driven by a coupling constant which is of the order of the inverse of the density of states. Finally, the dependence of the critical temperature on the electronic density depends on the change of the coupling constant with variations in the density of states, which is of the same order. Thus, no fine tuning of parameters is required to obtain corrections to the compressibility of the order of the compressibility itself.

The mechanism presented here is very general, and should play a role in many magnetic systems. Experimentally, the materials where it is best established are the "colossal magnetoresistence " compounds[17]. A number of observations[18, 19, 20] clearly suggest the existence of inhomogeneities and a domain structure at small scales, which is changed by the temperature (or the application of a magnetic field). Similar behavior has been observed in the pyrochlores[21], which form another family of compounds where a extremely large magnetoresistence near the Curie temperature has been observed.

A more indirect evidence of the tendency towards phase separation is the formation of ordered stripes in doped antiferromagnets. These stripes were first observed in doped nickelates[22], and later in the cuprates[23].

References

[1] P. B. Visscher, Phys. Rev. B **10**, 943 (1974).

[2] E. L. Nagaev, *Physica B* **230-232**, 816 (1997).

[3] J. Riera, K. Hallberg and E. Dagotto, *Phys. Rev. Lett.* **79**, 713 (1997).

[4] D. P. Arovas and F. Guinea, Phys. Rev. B **58**, 9150 (1998).

[5] S. Yunoki *et al.*, *Phys. Rev. Lett.* **80**, 845 (1998).

[6] E. Dagotto *et al*, *Phys. Rev. B* **58**, 6414 (1998).

[7] D. Arovas, G. Gómez-Santos and F. Guinea, Phys. Rev. B **59**, 13569 (1999).

[8] P. Majumdar and P. Littlewood, Phys. Rev. Lett. **81**, 1314 (1998).

[9] P. G. J. van Dongen, Phys. Rev. B **54**, 1584 (1996).

[10] C. S. Hellberg and E. Manousakis, Phys. Rev. Lett. **78**, 4609 (1997).

[11] E. W. Carlson, S. A. Kivelson, Z. Nussinov and V. J. Emery, Phys. Rev. B **57**, 14704 (1998).

[12] M. Imada, A. Fujimori and Y. Tokura, Rev. Mod. Phys. **70**, 1039 (1998).

[13] M. Calandra, F. Becca and S. Sorella, Phys. Rev. Lett. **81**, 5185 (1998).

[14] A. C. Cosentini, M. Capone, L. Guidoni and G. B. Bachelet, Phys. Rev. B **58**, R14685 (1998).

[15] F. Guinea, G. Gómez-Santos and D. Arovas, cond-mat/9907184 (preprint).

[16] We are thankful to D. Khomskii for pointing this out to us.

[17] J. M. D. Coey, M. Viret and S. von Molnar, Adv. in Phys. **48**, 167 (1999).

[18] J. de Teresa *et al*, Nature **386**, 256 (1997).

[19] M. Uehara *et al*, Nature **399**, 560 (1999).

[20] R. P. Borges *et al*, preprint.

[21] J. A. Alonso *et al*, Phys. Rev. Lett. **82**, 189 (1999)..

[22] C. H. Chen, Phys. Rev. Lett. **71**, 2461 (1993).

[23] J. Tranquada *et al*, Nature **375**, 561 (1995).